

Emplacement of volcanic vents and geodynamics of Central Anatolia, Turkey

D. Dhont ^{a,*}, J. Chorowicz ^a, T. Yürür ^b, J.-L. Froger ^c, O. Köse ^b, N. Gündoğdu ^b

^a *Département de Géotectonique, ESA-CNRS 7072, case 129, Université Paris 6, 4 place Jussieu, 75252 Paris cedex 05, France*

^b *Department of Geology, Hacettepe University, Beytepe, Ankara, Turkey*

^c *Centre de Recherches Volcanologiques, Université Blaise Pascal, 5 rue Kessler, 63038 Clermont Ferrand, France*

Abstract

Observations on Synthetic Aperture Radar (SAR) scenes of the European Remote Sensing (ERS) satellite and Digital Elevation Models (DEMs), complemented by field structural analysis permit a new understanding of relationships between tectonics and volcanism since the late Miocene (10 Ma) in Central Anatolia. Volcanic edifices form elongate stratovolcanoes, linear clusters and volcanic ridges. They indicate emplacement on tension fractures and tail-crack or horsetail features. For instance, the Kara Dag volcano is rooted on a tail-crack which accommodates a horizontal left-lateral throw component at a fault termination. Caldera complexes of Cappadocia are associated with horsetail fault patterns. The emplacement of volcanoes also benefits from larger-scale tectonic structures: the Erciyes Dag volcano is localized by the Sultan Saz releasing bend which opens along the sinistral strike-slip Ecemis fault. Deformation has been analysed from tension fractures—which are perpendicular to the direction of extension—and from field structural analysis. On a regional scale, the tectonic regime responsible for the distribution of volcanic vents in this area of convergence and lateral extrusion, is not compression but extension. The Central Taurus range is the thermally uplifted shoulder of the Adana–Cilicia basin, which is related to lithosphere thinning. Westward movements in the northwestern part of the studied area are influenced by the active back-arc Aegean extension situated to the west. Farther to the south, the direction of motion turns southwest and south, under the influence of the opening of the Adana–Cilicia basin. We interpreted that extension in the Central Anatolian plateau is related to crustal blocks moving above sub-horizontal detachment surfaces located in the lower crust. This is based on several facts: the Tuz Gölü fault zone is a within-crust detachment; the Tuz Gölü basin does not affect the whole lithosphere because otherwise it would have been bordered by thermally uplifted shoulders; movements change trend within a small (50 km) region. © 1998 Elsevier Science B.V. All rights reserved.

Keywords: Central Anatolia; Taurus; neotectonics; volcanism; tension fractures; detachment; satellite imagery; DEM; fault mechanisms

1. Introduction

Observation of geometric relationships between volcanism and tectonics is a fruitful approach in geology. On one hand, analysis of the distribution

and types of volcanic vents provides information on the geodynamics (e.g., Dengo et al., 1970; Stoiber and Carr, 1973; Nakamura, 1977; Hamilton, 1979; Chotin et al., 1980; Francis, 1993). On the other hand, tectonic analysis explains the location of volcanic vents, related for instance to tension fractures (e.g., Nordlie, 1973; Opheim and Gudmundsson, 1989; Takada, 1994; Koyaguchi and Takada, 1994;

* Corresponding author. Tel.: +33-1-44275089; Fax: +33-1-44275085; E-mail: damien@lgs.jussieu.fr

Chorowicz et al., 1997), fissures (e.g., Macdonald, 1972), pull-apart structures (e.g., Bellier and Sebrier, 1994), rifting (Smith et al., 1995) or reactivation of ancient faults (N'ni et al., 1986; Deruelle et al., 1987; Brousse and Lefèvre, 1990).

Recent and active tectonic and volcanic features have distinct geomorphic expressions. High ground resolution (10–30 m) satellite images and Digital Elevation Models (DEMs) express the landforms and yield synoptic views, permitting detailed mapping over large surfaces. Shadowed DEM images have proved to be efficient in structural analysis (Chorowicz et al., 1995a,b). Images acquired by the Synthetic Aperture Radar (SAR) of the European Remote Sensing (ERS) satellite are particularly sensitive to variations in ground slope.

The Central Anatolian region in Turkey (Fig. 1A) has been subjected to deformation and volcanism over the past 10 Ma (Innocenti et al., 1982; Sengör et al., 1985; Pasquarè et al., 1988; Aydar, 1992; Temel, 1992; Aydar et al., 1993; Le Pennec et al., 1994). This region is part of the Anatolia block which is moving westward by lateral extrusion as a consequence of north–south convergence between Africa–Arabia and Eurasia (McKenzie, 1972; Sengör et al., 1985; Dewey et al., 1986). The aim of this paper is to analyze the emplacement of volcanic vents and tectonics in Central Anatolia, using satellite and DEM images, complemented with field structural analysis. We shall argue that regional volcanism in Central Anatolia is associated with extension, not compression.

2. Regional structural framework

2.1. Geodynamic context

Convergence between Africa–Arabia and Eurasia (Fig. 1A) began in the mid-Cretaceous at around 100 Ma (Biju-Duval et al., 1977; Livermore and Smith, 1984; Yazgan and Chessex, 1991), inducing Campanian–Maestrichtian (~ 70 Ma) obductions over Ana-

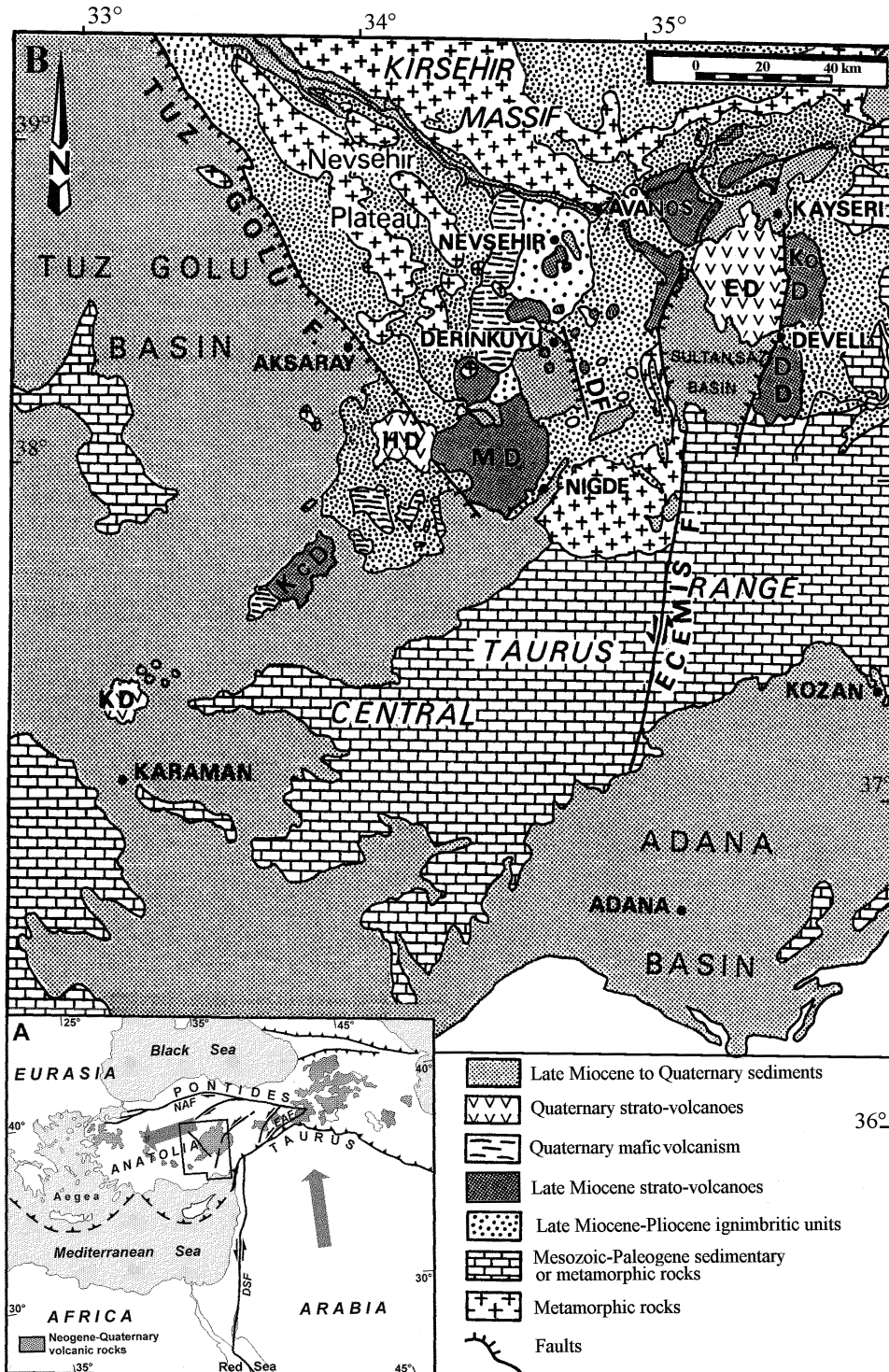
tolia and Africa–Arabia, and Eocene–early Oligocene (~ 30 Ma) collision and emersion in the Pontides (Sengör and Yilmaz, 1981). Red Sea continental rifting and individualization of Arabia began at the Oligocene–Miocene boundary (Le Pichon and Gaulier, 1988). In the mid-Miocene (~ 13 Ma), initiation of left-lateral motion along the Dead Sea Fault zone occurred (Joffe and Garfunkel, 1987), coeval with collision in the Eastern Taurus and related westward lateral extrusion of Anatolia bounded by the North and East Anatolian faults (McKenzie, 1972; Dewey et al., 1973; Sengör and Kidd, 1979; Sengör and Yilmaz, 1981; Yilmaz, 1993). Subduction in the Aegean region initiated during the late Miocene (Le Pichon and Angelier, 1979; Lyberis, 1985). We shall consider the late Miocene (~ 10 Ma) to present-day time globally and take into account only finite displacements and deformation during this interval.

2.2. Regional geology

The most prominent recent tectonic features of the studied area are the Tuz Gölü and Eceemis fault zones, the Central Taurus range and the Adana basin (Fig. 1B). They overprint crystalline and Mesozoic–Paleogene sedimentary or metamorphic rocks deformed in late Eocene–early Oligocene times (~ 30 Ma) by folds, thrusts and transcurrent faults.

Volcanism in Central Anatolia has developed since the late Miocene (Innocenti et al., 1975, 1982; Pasquarè et al., 1988). This volcanism has been considered to be related to compression (Pearce et al., 1990; Yilmaz, 1990) but it may also be the consequence of regional extension (Temel, 1992). It has mainly produced calc-alkaline rocks (Innocenti et al., 1982) and has been interpreted as an arc related to the north-dipping oceanic slab of the African plate (Innocenti et al., 1975, 1982) (Fig. 1A). The volcanics comprise late Miocene stratovolcanoes (e.g., Melendiz Dag), late Miocene–Pliocene ignimbritic units of Cappadocia (Le Pennec et al.,

Fig. 1. (a) Geodynamic context of Central Anatolia since the late Miocene. Large arrows show Africa–Arabia and Anatolia plate motions relative to Eurasia. Thick lines: plate boundaries. Rectangle: location of (b). DSF: Dead Sea Fault; EAF: East Anatolian Fault; NAF: North Anatolian Fault. (b) Geologic sketch map of Central Anatolia, compiled from the 1/2,000,000 geological map of Turkey (MTA, 1989). DD: Develi Dag volcano; DF: Derinkuyu fault; ED: Erciyes Dag; HD: Hasan Dag; KD: Kara Dag; KcD: Karaca Dag; KoD: Koç Dag; MD: Melendiz Dag.



1994), Quaternary stratovolcanoes (e.g., Erciyes Dag, Hasan Dag) and scattered vents of mafic or acidic volcanism.

The NW-striking Tuz Gölü fault zone forms the northeastern boundary of the Tuz Gölü basin (Arikan, 1975; Görür et al., 1984; MTA, 1989), situated at mean elevation 1000 m. The basin forms a northeast-dipping half-graben, infilled with 2000 m of Neogene sediments and volcanics, lying above several thousand meters of Eocene–Oligocene sediments. Southwest of the Hasan Dag volcano, the Tuz Gölü basin is partly overlain by volcanoes which form a NE-trending belt that extends as far as the Kara Dag stratovolcano in the SW. The Tuz Gölü basin is bordered to the northeast by the Nevşehir plateau and the Kirsehir massif, with crystalline basement rocks at mean elevations up to 1200 m, overlain by volcanic materials up to 2700 m at the summit of the Melendiz Dag.

The Ecemis fault zone strikes northeasterly in the north and turns around the transtensive (Pasquarè et al., 1988) Sultan Saz basin to strike NNE further south where it cuts the Central Taurus range. The Ecemis fault zone comprises in the south a narrow (1 km) strip of Paleocene(?)–Lutetian marl and sandstone, interbedded with clastic and detrital marine limestone, disconformably overlain by Oligocene to Quaternary continental detrital and evaporitic rocks (Yetis, 1984). The Ecemis fault zone cuts thrust-units emplaced during the late Eocene–Oligocene (~ 30 Ma) compressive event. It may have accommodated about 80 km of left-lateral slip motion since the Eocene and is considered to be still active (Özgül, 1976; Scott, 1981; Sengör and Yilmaz, 1981).

The Central Taurus range has been raised since the late Miocene (Özgül, 1976). It is made up of marine lower to middle Miocene sediments now at elevations of more than 2000 m, which unconformably overlie ophiolites and platform carbonate rock units thrust during the Late Eocene–Early Oligocene (~ 30 Ma) event.

The Adana basin is partly filled with turbiditic rocks spanning from Aquitanian to Tortonian (24–8

Ma), deposited in the zone where the African plate is subducting underneath Anatolia (Jackson and McKenzie, 1984; Karig and Kozlu, 1990). These rocks are overlain by Messinian (~ 6 Ma) evaporites and Pliocene (~ 5–2 Ma) marine sediments (Kelling et al., 1987). The basin emerged from below sea-level in the Quaternary but remains a low plain. In late Miocene–Plio-Quaternary time (since ~ 10 Ma), the Adana basin may be regarded as a pull-apart (Sengör et al., 1985; Dewey et al., 1986) or a releasing bend basin (Chorowicz et al., 1994a,b), developed along faults which mark the prolongation of the left-lateral East Anatolian fault, related to the lateral expulsion of Anatolia (Fig. 1A).

According to Sengör et al. (1985), Central Anatolia presently undergoes moderate NE–SW-trending compression, but Pasquarè et al. (1988) and Toprak and Göncüoğlu (1993) have associated the Central Anatolia grabens with a late-Miocene to early Pliocene (~ 10–4 Ma) east–west-trending tension. Pasquarè and Ferrari (1993) and Borgia et al. (1994) have suggested that there is a N-trending, 100-km-long, buried graben in the central part of the Nevşehir plateau and that the Tuz Gölü and Ecemis faults are reverse faults formed as a result of the intrusion of a large batholith.

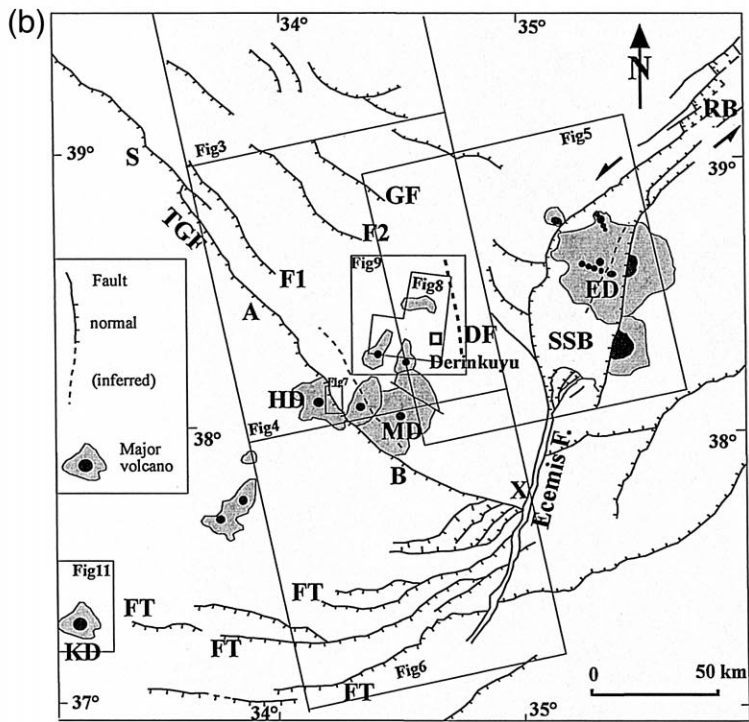
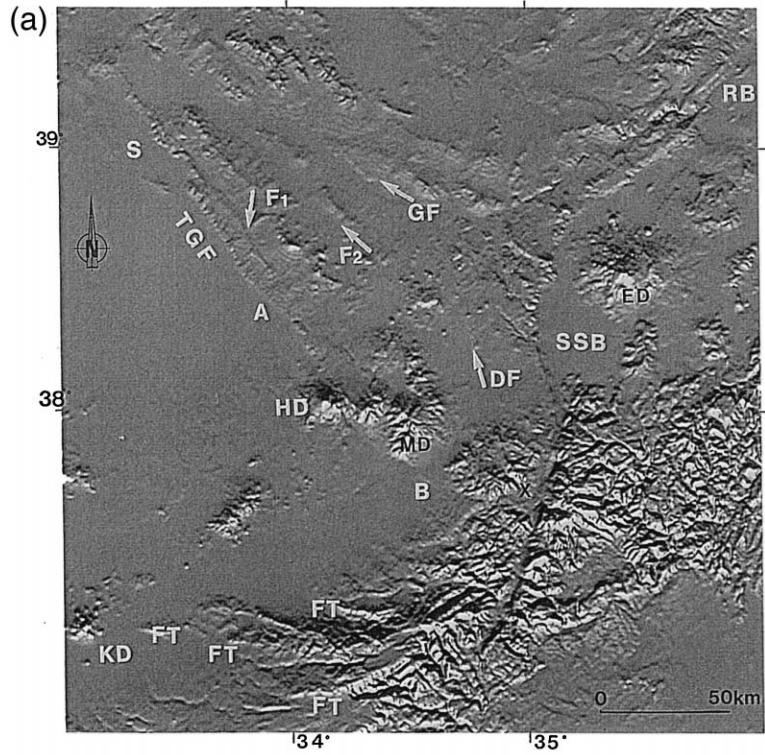
3. Data and methodology

3.1. Data

A DEM of the whole area has been developed using a kriging method, from the digitization of elevation contour lines (25 to 100 m vertical contour intervals) of nine topographic maps at 1/250,000 scale. It covers 260 × 320 km with 500 m horizontal ground resolution (Fig. 2).

We have analyzed four ERS-1 SAR images (Figs. 3–6). We applied standard processing to generate an image from each original digital scene covering 100

Fig. 2. Shadowed image (a) of the DEM of the studied area, at 500 m horizontal ground resolution, illuminated from south, and structural interpretation (b). A: Aksaray; B: Bor; DF: Derinkuyu fault; ED: Erciyes Dag; F1 and F2: inactive faults; FT: normal faults of the Central Taurus range; GF: Gumuskent fault; HD: Hasan Dag; KD: Kara Dag; MD: Melendiz Dag; RB: rhomb shaped basins; S: Sereflikoçhisar; SSB: Sultan Saz basin; TGF: Tuz Gölü fault. X: the Tuz Gölü fault terminations against the Ecemis fault.



× 100 km, at 25 m ground resolution. Illumination is from the WSW. We have produced negative prints in order to express in black the slopes facing the radar source. Detailed information is well revealed by

various gray tones on the slopes backing the illumination.

High ground resolution (10 m) panchromatic SPOT images have also been processed in order to

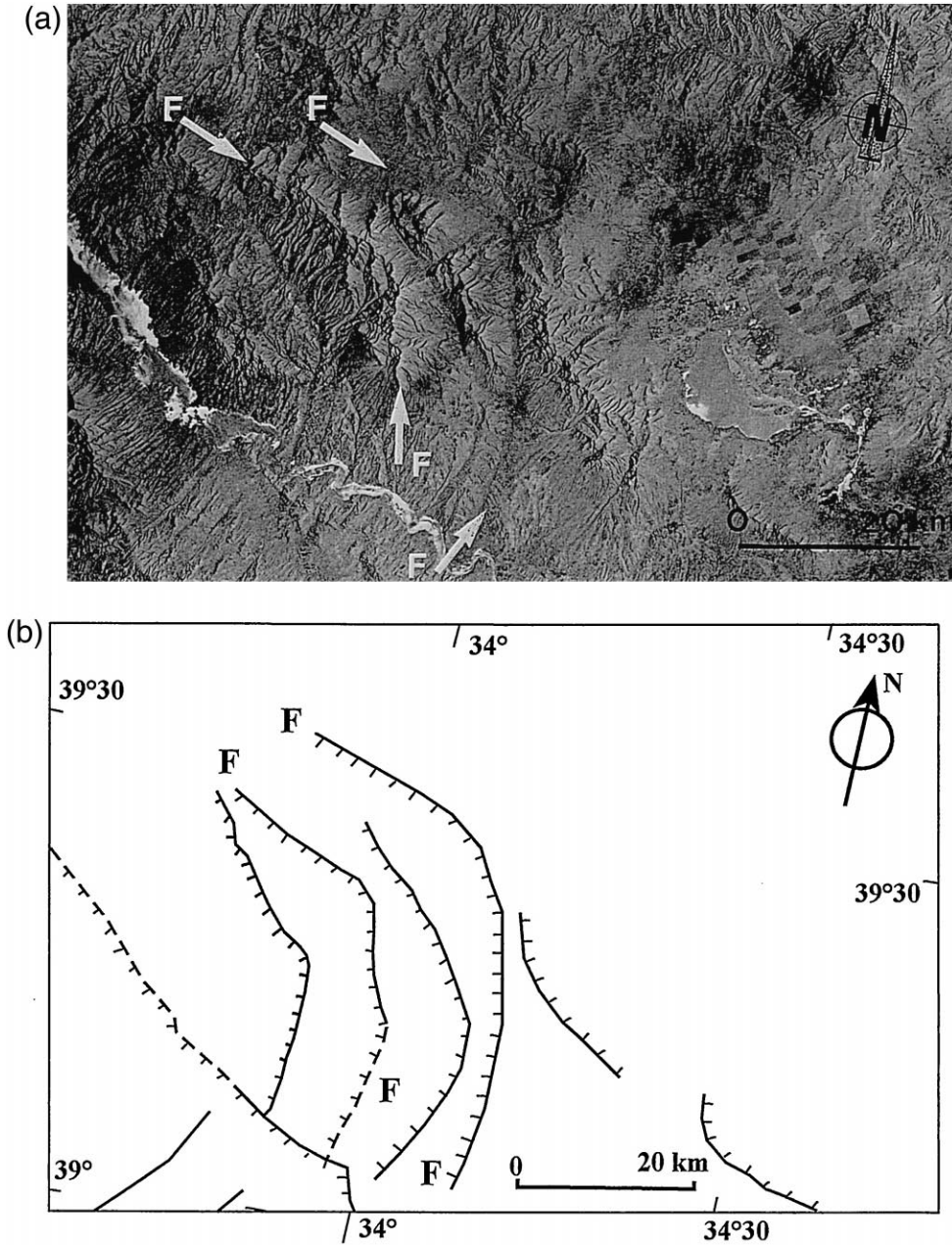


Fig. 3. SAR ERS-1 image (negative view) of the Nevsehir plateau and Kirsehir massif (a) and structural interpretation (b). F are curved faults in plan view, interpreted as extensional spoon faults. Location on Fig. 2.

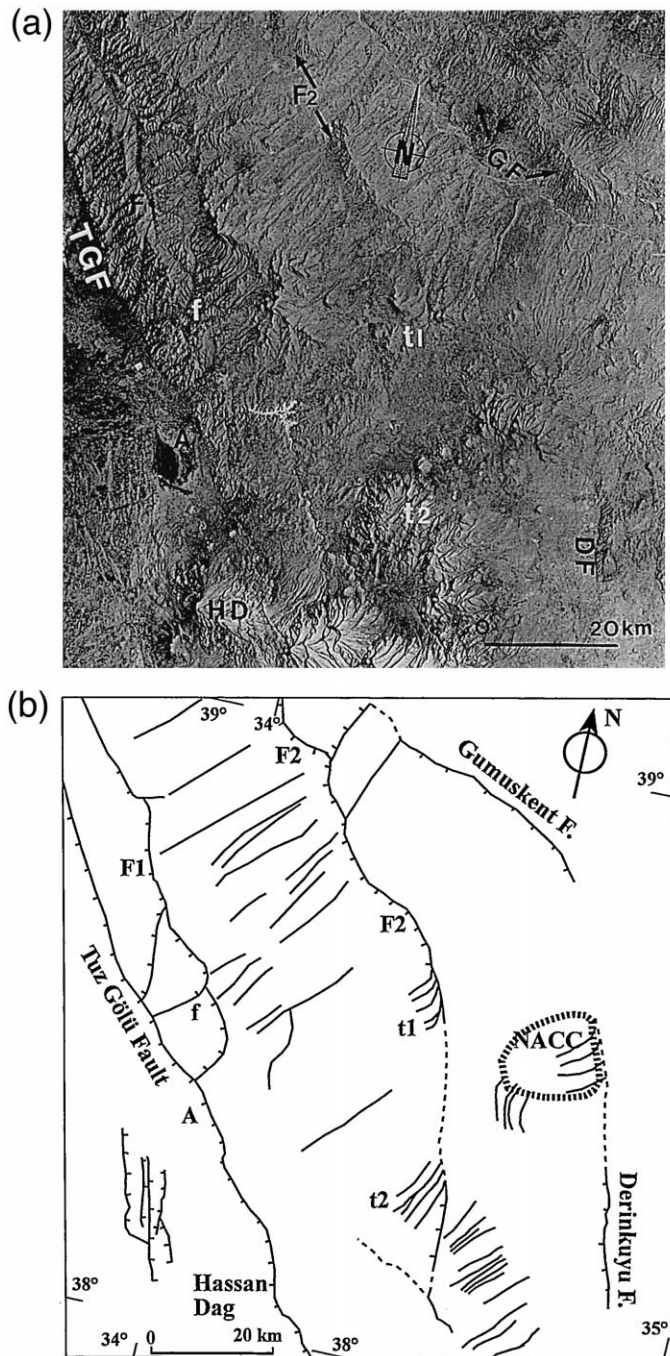
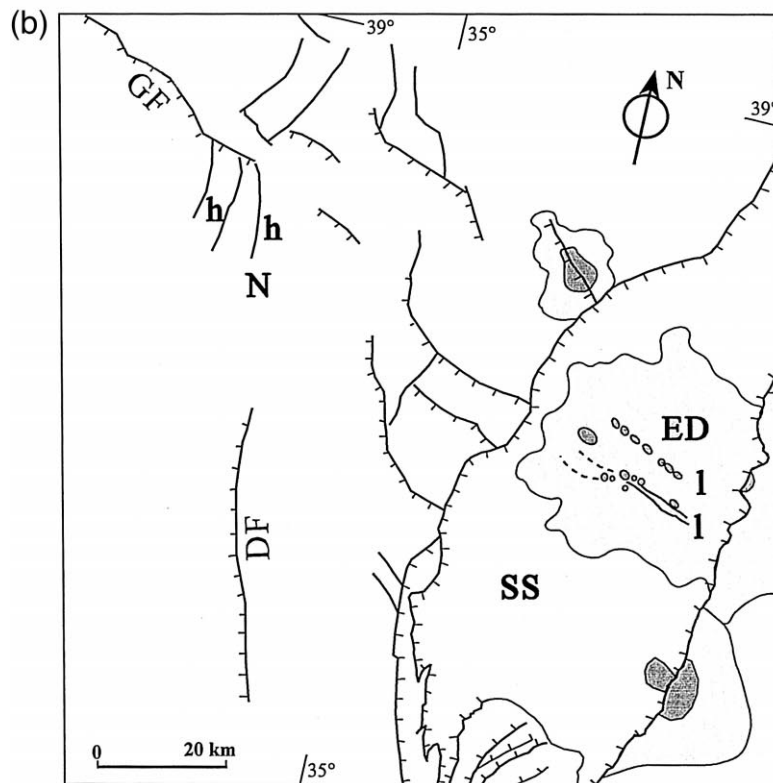
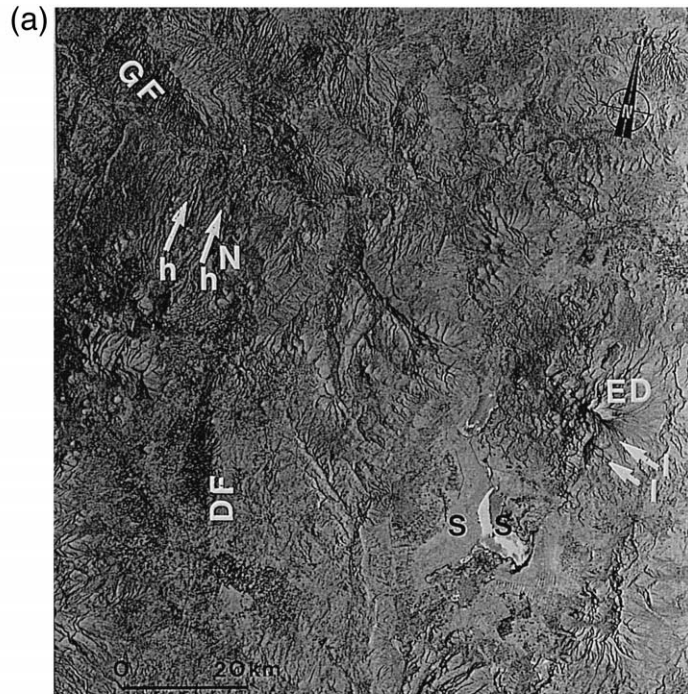


Fig. 4. SAR ERS-1 image (negative view) of the Tuz Gölü fault (TGF) area (a) and structural interpretation (b). A: Aksaray; DF: Derinkuyu fault; F1 and F2: inactive faults; f: curved faults in plan view at southeastern termination of fault F1; GF: Gumuskent fault; HD: Hasan Dag; NACC: Nevşehir–Acıgöl Caldera Complex; t1 and t2: horsetail structures. Location on Fig. 2.



obtain detailed views of particular areas. We have mainly used scene KJ 113–273 (Fig. 7) and KJ 114–272 to make a small mosaic (Fig. 8).

3.2. Methodology

Observations from ERS-1 SAR, SPOT and DEM images have been used to map the recent faults and locate the volcanic vents. These features have been consolidated onto a single map (Fig. 9).

Recent faults interpreted as active or inactive are determined from their distinct, poorly eroded scarp or because they affect the recent ($\sim 10\text{--}0$ Ma) rocks. We systematically have compared our images with geological maps in order to carefully separate the scarps formed by fault planes (active) from those resulting from differential erosion of contrasted lithology (ancient). In some cases, Quaternary deposits overlie the fault trace which is in the prolongation of distinct scarps, as is the case for the Gumuskent–Derinkuyu fault (Fig. 9). This pattern indicates that the fault is recent but inactive.

We have specially searched for the volcanic vents and related volcanic cones or craters. Following Nordlie (1973), we have considered the outlines of lowermost floors of volcanic edifices, which are generally horizontal. Some volcanoes and craters are clearly elongate. Aligned and adjacent volcanoes define what we refer to as volcanic linear clusters (Takada, 1994; Gudmundsson, 1995). Elongate volcanoes and volcanic linear clusters are related to hidden tension fractures which permit lavas to reach the surface (Chorowicz et al., 1997). Tension fractures are perpendicular to the direction of extension. On the map of Fig. 9, we have drawn the tension fractures inferred from elongate volcanoes and volcanic linear clusters and have indicated the direction of local extension.

To complement this information relative to the strain, we have carried out structural analysis in the field, searching for local slip movements along the main faults and for local strain or paleostress patterns. Our observations consisted of measurements of tension fractures and orientations and sense-of-mo-

tion of striated fault planes (Fig. 10). Special emphasis has been placed on striations directly observed on the major mapped fault planes, on which the main part of the regional displacements occurred. We have also taken into account striations observed on smaller faults paralleling the nearby major fault, assuming that in a given local stress field parallel faults have the same mechanism, for a given tectonic phase. We have plotted on the trace of the main faults the plunge of striations, with indications of the sense of movement (Figs. 9 and 10). Along the major faults we have generally found only one set of striations which we assume to be related with the latest displacements. In a few sites not located along major mapped faults, we have used striations on the various minor fault surfaces to estimate the orientation of the local paleostress pattern, using the right dihedral method of Angelier and Mechler (1977). We considered that all measurements from any one site are related to a single finite deformation and paleostress pattern unchanged since 10 Ma. The fact that the results of our calculations are consistent from place to place throughout the Central Anatolian region justifies this hypothesis. However, when two deformation events were supposed to have occurred, because of incompatibilities in the data or several striation sets on fault planes, the measurements were sorted by relative age at each site. To characterize the paleostress at each site, we used parameter $[(\sigma_2 - \sigma_3)/(\sigma_1 - \sigma_3)]$ which ranges from 1 to 0. The stress ellipsoid has three well distinguishable axes when values of this parameter are close to 0.5. Values approaching 0 indicate that σ_3 is equal to σ_2 .

4. Structural observations

4.1. Tuz Gölü structure

4.1.1. Tuz Gölü fault zone

The main Tuz Gölü fault trace (Fig. 9), well expressed on the DEM (Fig. 2) and SAR or SPOT images (Figs. 4 and 7) cuts the Quaternary Hasan

Fig. 5. SAR ERS-1 image (negative view) (a) and structural interpretation (b) of the Sultan Saz basin (SS) and part of the Cappadocia region, including the Gumuskent and Derinkuyu faults (GF and DF). h: NNE-striking faults south of Nevşehir (N) forming a horsetail pattern. l: NW-SE structural lines affecting the Erciyes Dag (ED). Location on Fig. 2.

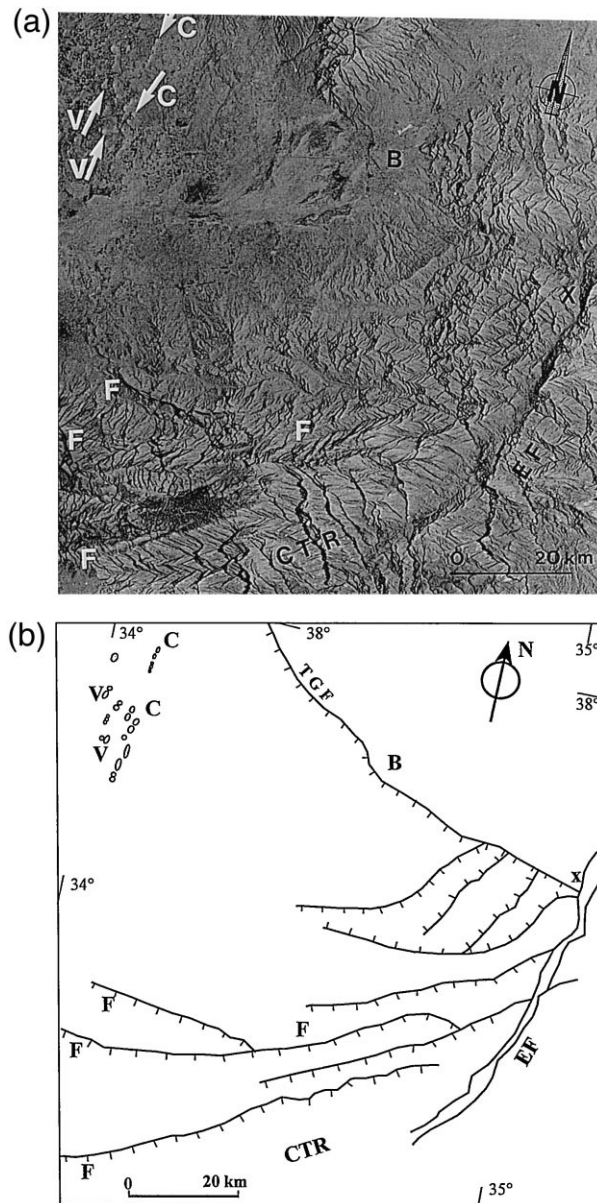


Fig. 6. SAR ERS-1 image (negative view) of part of the Central Taurus (a) and structural interpretation (b). B: Bor; C: linear clusters of volcanoes; CTR: Central Taurus range; EF: Ecmis fault; F: normal fault; X: termination of the Tuz Gölü fault against the Ecmis fault; V: elongate volcanoes. Location on Fig. 2.

Dag stratovolcano, attesting to recent movements (Aydar, 1992; Toprak and Göncüoğlu, 1993). The main crater of Hasan Dag is not on the fault but 8 km away (Fig. 2). Both DEM and SAR imageries clearly indicate the Tuz Gölü fault extends southeast-

ward, up to the point where it ends against the Ecmis fault (X on Figs. 2 and 6). The Tuz Gölü fault dips \sim SW 65° in sites 1 and 4 (Fig. 10). Striations on the main fault plane are indicative of W-oriented oblique-slip dextral transpressive dis-



Fig. 7. Window of SPOT image KJ: 113–273, showing lava flows of the Quaternary Hasan Dag stratovolcano offset or confined by the Tuz Gölü fault (TGF) which trace is followed by arrows. Location on Fig. 2.

placements. Strike-slip paleostress regimes with σ_1 and σ_3 horizontal are recognized in sites 3 and 5 (Fig. 9), in Eocene beds. Several episodes, including the Quaternary one, appear to be represented, all of them yielding E–W to NW–SE σ_3 trend. Near Bor (sites 13 and 14, in late Miocene rocks), tension fractures and microfaults indicate NE- to ENE-trending, post late Miocene extension.

4.1.2. Tuz Gölü basin

A series of small Plio-Quaternary volcanic cones is visible in the northwestern corner of Fig. 6. Some are elongated in the N 10° direction (V on Fig. 6). Smaller volcanoes adjacent to each other form linear clusters, also trending N 10° (C on Fig. 6). The local Plio-Quaternary extension in sites 16 and 17 is consequently oriented N 100° (Fig. 9). In the field we have found small (200 m long, 20 m wide) volcanic ridges, a few meters higher than the nearby lava flow surface, trending N 00 to 20° (site 15 on Fig. 10). The volcanic ridges seem related to basalt filling

tension fractures which formed within still warm basalt flows, possibly related with Plio-Quaternary strain yielding E-trending extension (site 15 on Fig. 9).

The Kara Dag volcano is located near the southern termination of a SSE-striking fault, which turns SE at its southern end. The fault cuts the volcano into two parts which are slightly (100 m) left-laterally displaced (Fig. 11). The fault is mainly extensional, western side down. In site 2, striations on a small conjugate fault indicate oblique-slip movement with a left-lateral throw component (Fig. 10). In site 18 (Fig. 11), a 300-m-long and 50-m-wide fissure eruption was formed through a tension fracture striking N 140°, indicating N 50°-trending local extension. The Kara Dag is then rooted on a tail-crack feature which accommodates the horizontal left-lateral throw component at fault termination (Fig. 11). South and southwest of the volcano, in sites 19 and 20, linear clusters of central volcanoes and fissure eruptions respectively indicate N 50° and N 10 to 30° extension (Fig. 9).

4.1.3. Nevşehir plateau

The Tuz Gölü fault zone bounds on its southwestern flank a NE-dipping tilted block, comprising Eocene–Oligocene beds unconformably overlain by NE-dipping Pliocene sediments (MTA, 1989) (Figs. 2 and 4). Another NE-dipping tilted block is bounded by the F1 normal fault (Figs. 2, 4 and 9). F1 is inactive, the fault scarp being attenuated by erosion. We have observed in the field it is locally overlain by Quaternary sediments. F1 ends to the southeast in several strands, curved in plan view (f on Figs. 4 and 9). Another fault (F2), more or less parallel to the Tuz Gölü fault, is also partly hidden by Quaternary sediments, and consequently is regarded inactive (Figs. 2, 4 and 9). The fault trace comprises large curves and possible horsetail structures shown by arched ravines which do not follow the local maximal slope (t1 and t2 on Fig. 4). t2 is located at the center of the late Miocene–Pliocene Derinkuyu Caldera Complex (Fig. 9) which is evidenced by gravimetric data (Froger et al., 1998) but not visible on our images because covered by the ignimbrites.

The Gumuskent and Derinkuyu faults (respectively GF and DF on Figs. 2, 4, 5 and 9), running

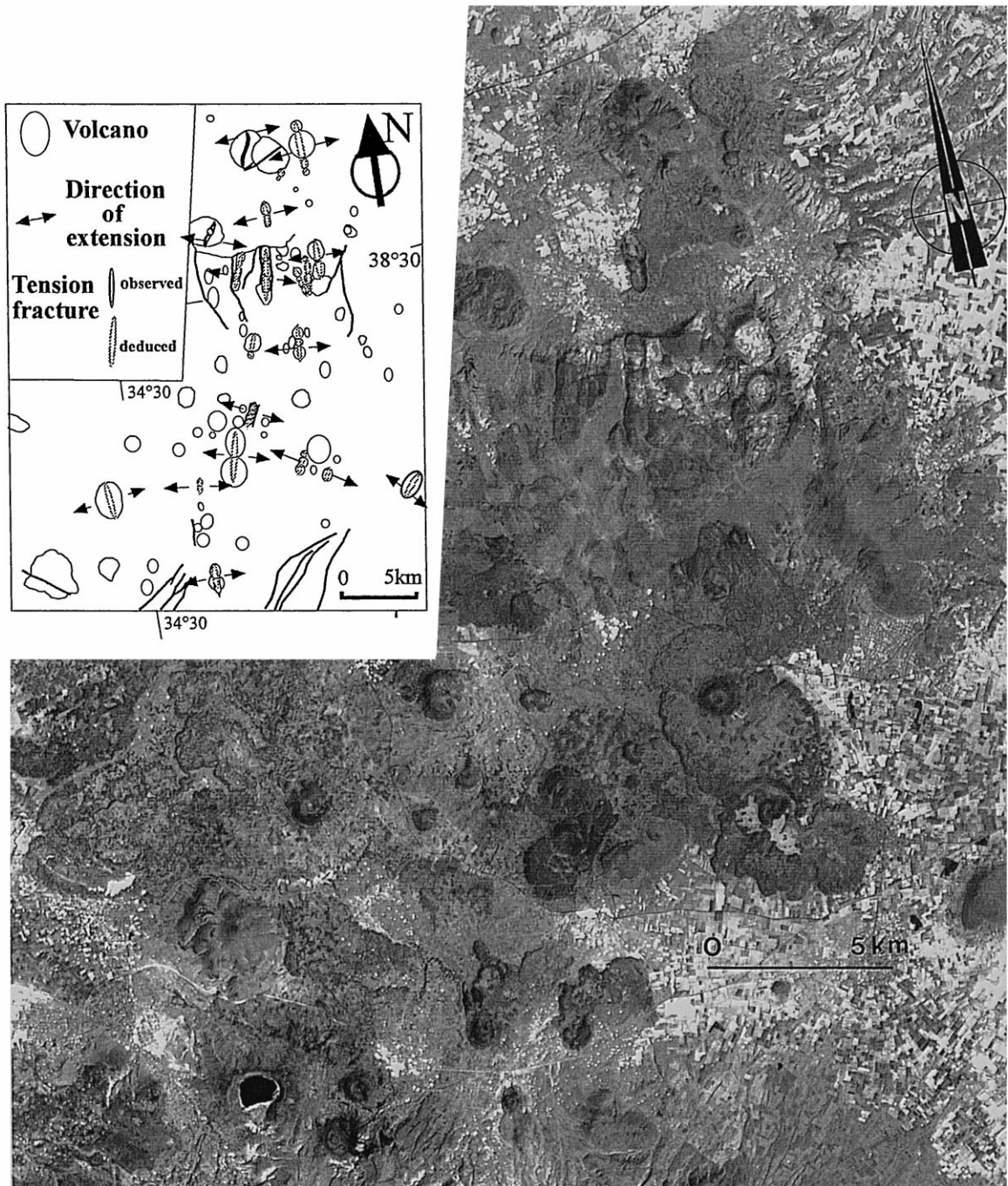


Fig. 8. Mosaic of windows extracted from two SPOT images (KJ: 113–273 and 114–272), covering the Quaternary volcanic field in the Derinkuyu area, Cappadocia. Inset shows the distribution of monogenic vents. Most of the vents are randomly distributed but some form linear clusters which we interpret as tension fractures, yielding E-trending direction of extension. Location on Fig. 2.

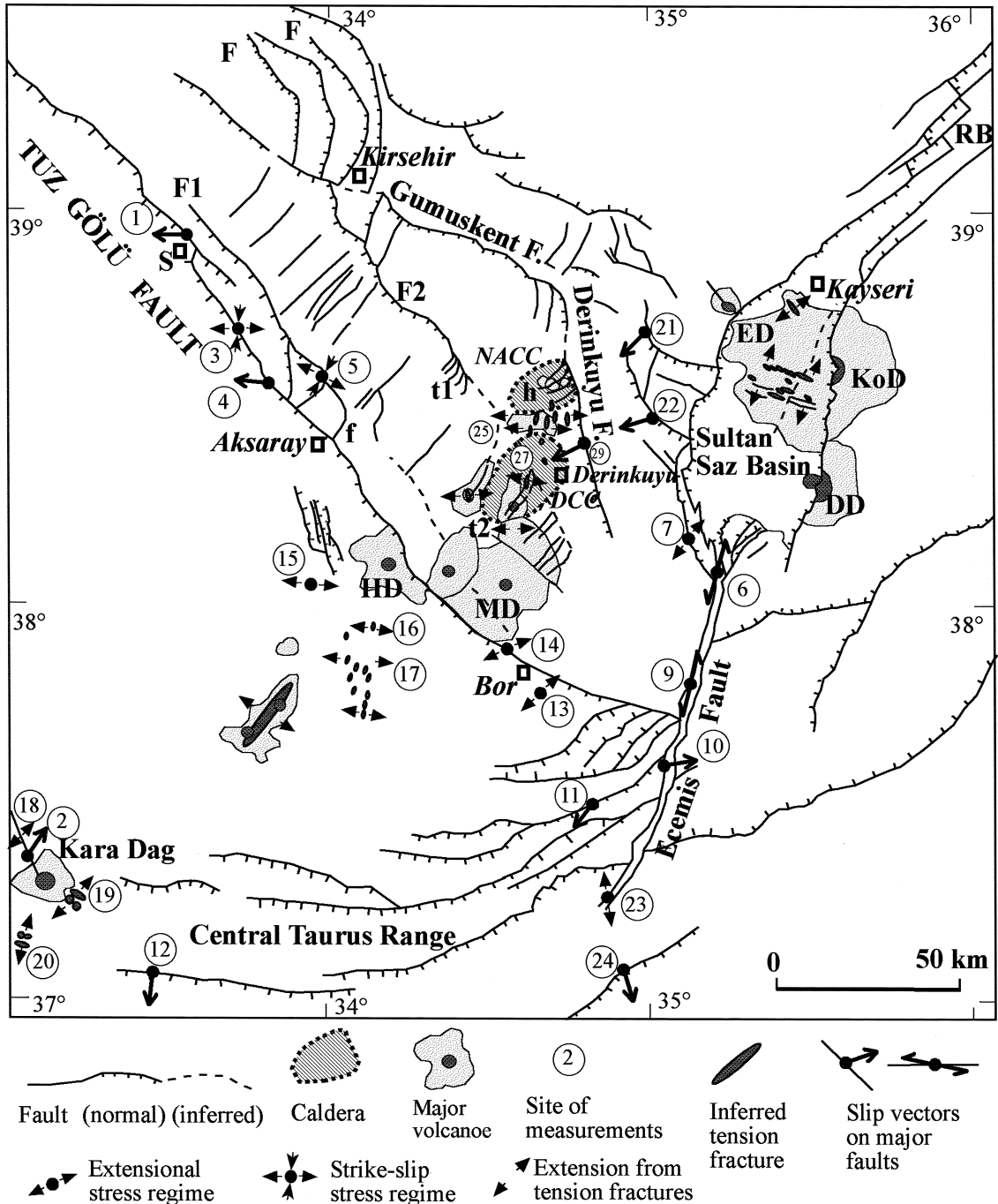


Fig. 9. Synthetic map of tectonic and volcanic features observed from all above data. DCC: Derinkuyu Caldera Complex; DD: Develi Dag; ED: Erciyes Dag; F: curved faults in plan view; F1 and F2: inactive faults; f: curved faults in plan view at southeastern termination of fault F1; h: horsetail pattern; HD: Hasan Dag; KoD: Koç Dag; MD: Melendiz Dag; NACC: Nevşehir–Acigöl Caldera Complex; RB: rhomb shaped basins; S: Sereflikoçhisar; t1 and t2: horsetail structure along fault F2. Number in circle are sites of structural analysis (see Fig. 10).

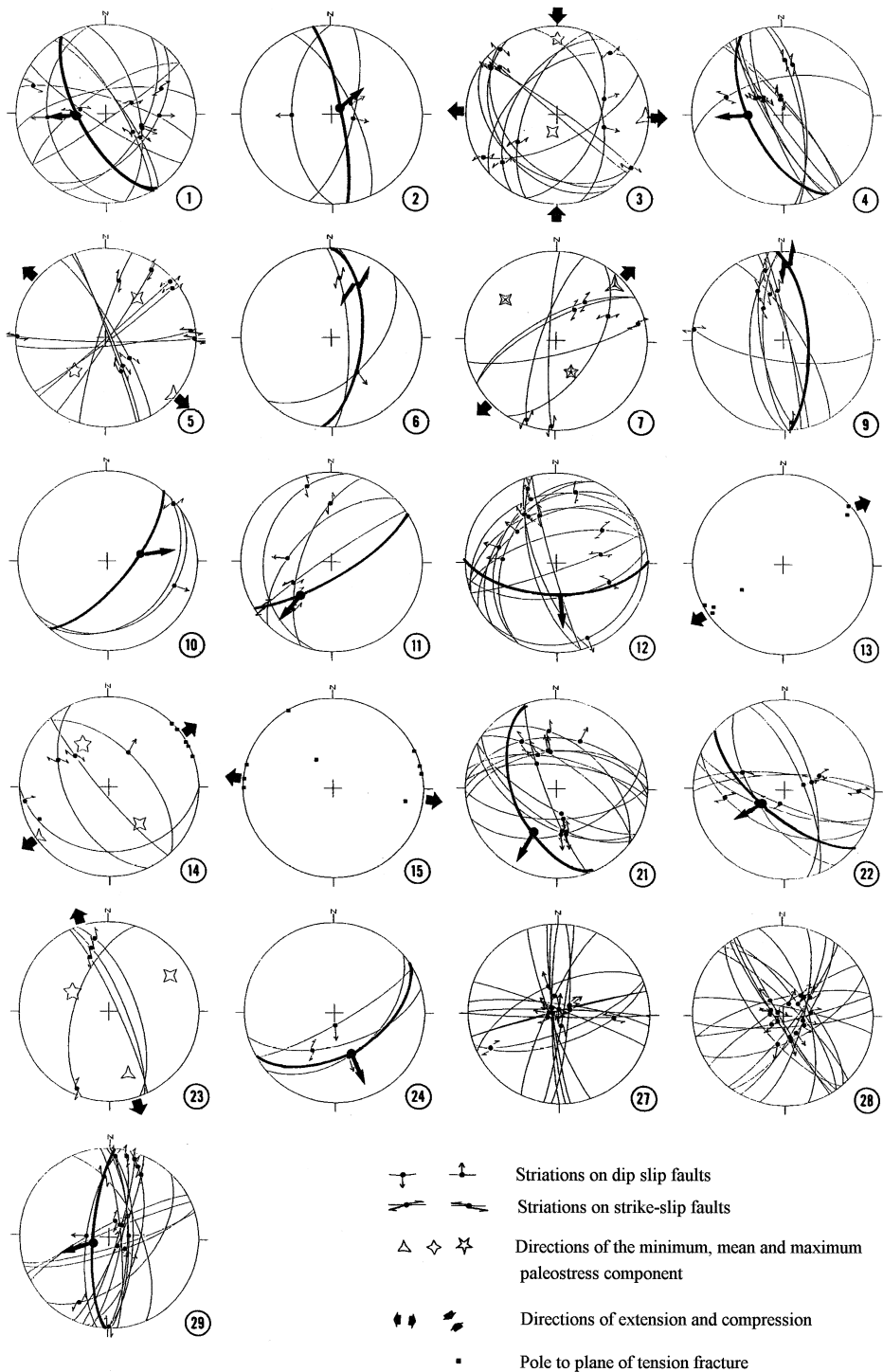


Fig. 10. Data from field structural analysis. Schmidt stereograms, lower hemisphere. Thick lines are major (mapped) fault planes and related striations. Sites (number in circle) are located on Fig. 9.

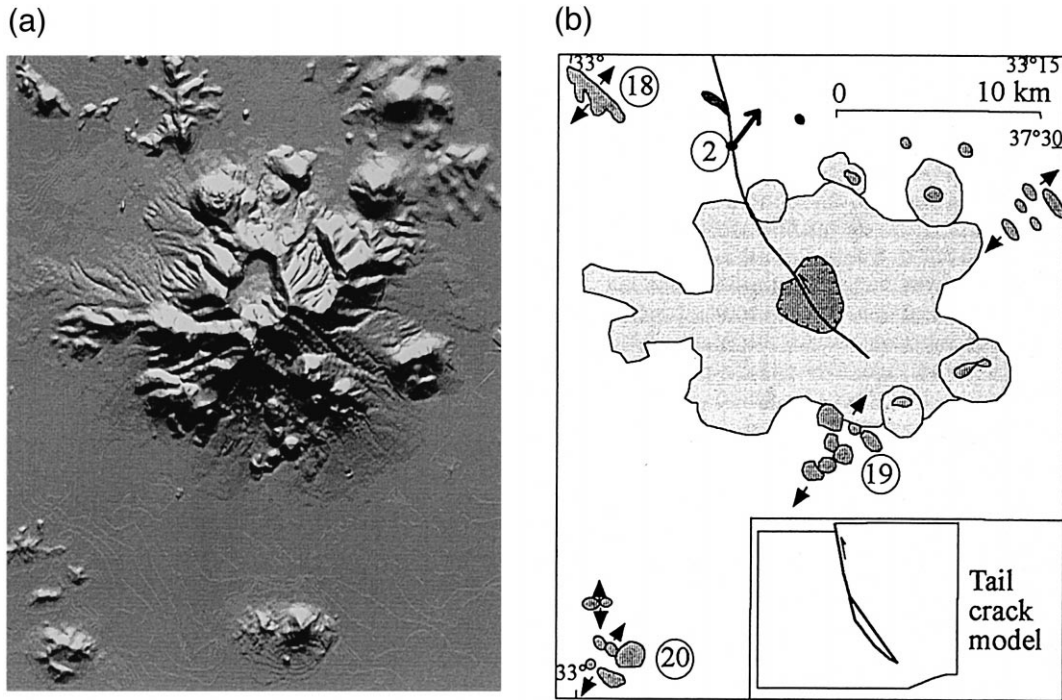


Fig. 11. Left: DEM image of the Kara Dag volcano region, illuminated from north. Location on Fig. 2. Right: interpretation of the DEM. Numbers in circle refer to locations cited in the text and plotted on Fig. 9. Opposite arrows indicate local extension direction perpendicular to volcanic ridges or linear clusters. The crater shape as well as striations in site 2 testify to left-lateral displacement component. The inset is a vertical view of the tail-crack model.

more or less parallel to the Tuz Gölü fault, are composed in plan view of curved segments. Gravimetric data have shown evidence (Froger et al., 1998) that the Gumuskent and Derinkuyu faults form a continuous line which we call the Gumuskent–Derinkuyu fault zone. Morphologic expression is poor in some places because these faults tend to be hidden by Quaternary volcanic materials. Southeast of Nevşehir, the fault line is very clear (Derinkuyu fault), possibly because it is still active. In site 29 (Fig. 9), striations on a small fault paralleling the main fault, dipping W 70° , indicate N 10° oriented horizontal relative displacement (Fig. 10). The Nevşehir–Acigöl Caldera Complex (NACC), evidenced by gravimetric data (Froger et al., 1998), appears on the ERS-1 SAR image of Fig. 4 as a depression surrounded by radial drainage pattern. The caldera is superimposed on a possible horsetail structure related to the Gumuskent–Derinkuyu fault. As is the case in Ethiopia (Chorowicz et al., 1994b),

we infer that there are relationships between a caldera and a tail-crack or horsetail pattern.

The Tuz Gölü, F1, F2 and Gumuskent–Derinkuyu faults are made of a succession of curved segments suggesting to us that they are southwest-dipping listric planes (spoon-faults). They are sub-parallel to each other. The Tuz Gölü fault only is active all along its line. The F1, F2 and Gumuskent–Derinkuyu faults are mostly inactive. We interpret that all these faults are related to the same in-depth detachment. The spoon-shaped extensional detachments seem to have migrated from the Gumuskent–Derinkuyu fault, successively to F2, F1 and finally to the presently active Tuz Gölü fault.

More to the northwest, the Kirsehir massif is cut by a series of faults (F on Fig. 3), bounding tilted blocks, which change strike progressively from SE to S and are cut by the Gumuskent and F2 faults (Fig. 9). Their shape in plan view is very arched and they can be regarded as listric (spoon faults). Given the

moderate size (10 km in width) of the tilted blocks the faults are not of lithospheric scale and they probably affect only part of the crust.

We have studied a SPOT image of a Quaternary volcanic field located in the northern side the Derinkuyu Caldera Complex (Fig. 8). Some of the volcanoes are either close or abut to each other, and are aligned N 00 to N 40°, forming linear clusters which we infer to be rooted on tension fractures. These trends indicate N 90 to N 130° extension (site 25 on Fig. 9). Many randomly distributed monogenetic volcanoes do not seem related to faults. Within the Derinkuyu Caldera Complex itself, at sites 27 and 28 (noted 27 on Fig. 9), the striated fault pattern is that of vertical displacements (paleostress ellipsoid has vertical σ_1 ; horizontal σ_2 and σ_3 are equal). We interpret this local brittle deformation to result from caldera collapse.

Northeast of Derinkuyu, there are several normal faults with curved traces, bounding tilted blocks (Fig. 2). Seismic activity in this area is marked by the earthquake which occurred in the area in 1938 [Kirsehir event in the work of Jackson and McKenzie (1984)]. For a NW-striking fault, the fault plane solution indicated oblique-slip dextral motion, compatible with site 22 (Figs. 9 and 10). Striations on major fault planes in sites 21 and 22 express SSW- and SW-directed displacements.

4.2. Ecemis fault zone

The Ecemis fault zone is well displayed on the DEM and SAR ERS images (Figs. 2 and 6). In the northern part of the studied area (RB on Fig. 2), it bounds elongate rhomb-shaped basins filled with Plio-Quaternary sediments, forming pull-apart basins related with left-lateral strike-slip motion along the fault zone.

Further south, the Ecemis fault progressively turns S and then SSE, around the Sultan Saz basin (Figs. 2 and 5). This geometry resembles that of a lazy-S-shaped releasing bend basin (Mann et al., 1990) formed along a left-lateral strike-slip fault. However, the Sultan Saz plain is larger than a simple releasing bend pattern, suggesting that the basin has increased in width by collapse of the borders. This interpretation is supported by the eastern border scarp made of a succession of smaller arched fault segments, in-

dicative of gravity collapse movements (Chorowicz and Sorlien, 1992), possibly also related with caldera growth. In the southern border, a set of NE-striking normal faults (Fig. 9) is possibly related to southward growth of the basin. A faint line visible on the DEM of Fig. 2, cutting across the Erciyes Dag volcano, may represent the main trace of the deep Ecemis fault. In this view, the releasing bend has not a typical shape. We interpreted that NE- to E-trending extensional strain south of Derinkuyu (Fig. 9) has compensated the opening which would have occurred in the southern part of the ideal releasing bend. Moreover, the FT branching faults (Fig. 2) give the false impression of a horsetail pattern indicating right-lateral slip component, but in fact these FT faults are related to extension in the Taurus and cannot be regarded as marking the end of the Ecemis fault. Volcanoes Erciyes Dag, Koç Dag and Develi Dag (Fig. 9) are located respectively within the releasing bend basin and along the eastern border fault. The Erciyes Dag volcanic edifice includes a WNW-trending succession of vents and faults (I on Fig. 5), probably superimposed on NW-trending tension fractures indicating SSW-directed extension.

Further south, the Ecemis fault zone forms a zigzag shaped corridor (Fig. 6). Straight scarps along the eastern fault are only slightly eroded, testifying to recent activity. In site 6 (Fig. 9), striations show that horizontal component of strike-slip displacement is oriented N 20° (Fig. 10). In Neogene tuff and conglomerate at site 7, the σ_3 paleostress component trends N 40°. Site 9, in Oligo-Miocene conglomerate and reddish clay, located close to the main fault (Fig. 9), indicates left-lateral strike-slip movement. These three sites argue SSW-directed motion and left-lateral mechanism along the Ecemis fault. Local (collapse?) movements may occur as is the case for site 10, in Quaternary alluvial terrace gravel, close (100 m) to the main fault, where transtensional displacement is oriented N 80°.

4.3. Central Taurus range

On the DEM (Fig. 2) and SAR (Fig. 6) images we have observed that the Ecemis fault zone connects to the southwest in the Central Taurus range with a series of faults which die out westward (FT on Fig. 2 or F on Fig. 6). These faults have been plotted on a

topographic cross-section (Fig. 12b). They bound north-dipping tilted blocks and are extensional. In site 12, we have observed a large fault affecting marine early-middle Miocene layers and their basement (Figs. 9 and 10). The fault is normal dip-slip and attests to recent local N–S extension. In site 11, extensional oblique-slip faults reactivate ancient thrust faults and testify to recent SW-directed horizontal displacement (Fig. 10). In site 24 (Fig. 9), relative extensional displacement is directed N 160° (Fig. 10). Measurements in site 23 give a N 165° trending σ_3 . We conclude that the present-day Central Taurus belt, unlike the Eastern Taurus, is not compressive but is under tension. Elevations in the Central Taurus are the highest in the studied area (Fig. 12a), except for major volcanoes. These high mountains do not result from compression, as is the case in the Eastern Taurus. The last compression event in this area consequently occurred in the late Eocene.

5. Discussion

5.1. Distribution of volcanic vents

Most volcanic vents such as volcanic ridges, linear clusters and isolated stratovolcanoes are interpreted to be rooted on tension fractures. We show below that other open structures are able to give way for the magma. Many monogenetic volcanoes are randomly distributed but we think that each of these volcanoes is rooted on a tension fracture as is the case in Iceland (Chorowicz et al., 1997).

The Kara Dag structure (Fig. 11) is an example of central volcano rooted on a tail-crack opening at oblique-slip fault termination. The tail-crack model can be extended to other strike-slip or oblique-slip faults which open termination has given way to volcanic materials. Caldera complexes near Derinkuyu (Fig. 9) are associated with horsetail structures developed at the termination or along major faults. The Derinkuyu Caldera Complex is located at the southeastern end of fault F2, where a horsetail structure occurs (t2 on Fig. 9). A horsetail pattern can be considered equivalent to several tail-cracks at a fault termination or partial termination.

The Nevşehir–Acigöl Caldera Complex is not at a fault end but rather slightly apart from the Gumuskent–Derinkuyu fault line. However, a set of NNE-striking faults occurs, forming a horsetail pattern (h on Figs. 5 and 9). We interpret that the late Miocene Gumuskent–Derinkuyu fault line ended into the horsetail pattern (h), accommodating part of the right-lateral strike-slip component. The fault line now continues into the active Derinkuyu fault.

Another way for the magma to reach the surface is at a deep-seated releasing bend opening along a strike-slip fault zone. This seems to be the case in the Sultan Saz basin for the Erciyes Dag and perhaps for the Koç Dag and Develi Dag volcanoes. However, the Erciyes Dag is also rooted on NW-striking tension fractures. At the regional scale, the central volcano may benefit from the releasing bend opening, but at local scale emplacement is related to tension fractures.

The Hasan Dag volcano is situated close to the Tuz Gölü fault, near a sharp change in strike forming a right-stepping dog-leg feature (Figs. 4 and 9). The fault having a right-lateral strike-slip component, the dog-leg is likely to make a small releasing bend opening. We did not find on Fig. 4, at the location of Hasan Dag, intersections of the Tuz Gölü fault with other faults as indicated by Toprak and Göncüoğlu (1993). We consider that the volcano has benefited from a small releasing bend opened along the Tuz Gölü fault, but that its local emplacement is possibly related to a tension fracture.

Finally, emplacement of volcanoes can be regarded at several scales. On a regional scale, there is no compression, and extension can be considered to be responsible for volcanism. At the local scale, the emplacement of vents is controlled by tension fractures, tail-crack or horsetail features, but volcanoes also seem to be sometimes localized by larger scale tectonic structures such as releasing bends along strike-slip or oblique-slip faults.

5.2. Tectonics

Elevations in the Central Taurus range (Fig. 12a), progressively decrease westwards, with the dying out of large normal faults and tilted blocks. We associate this with location near the southwestern end of the Adana basin (Fig. 1). Offshore data indicate a 1000-

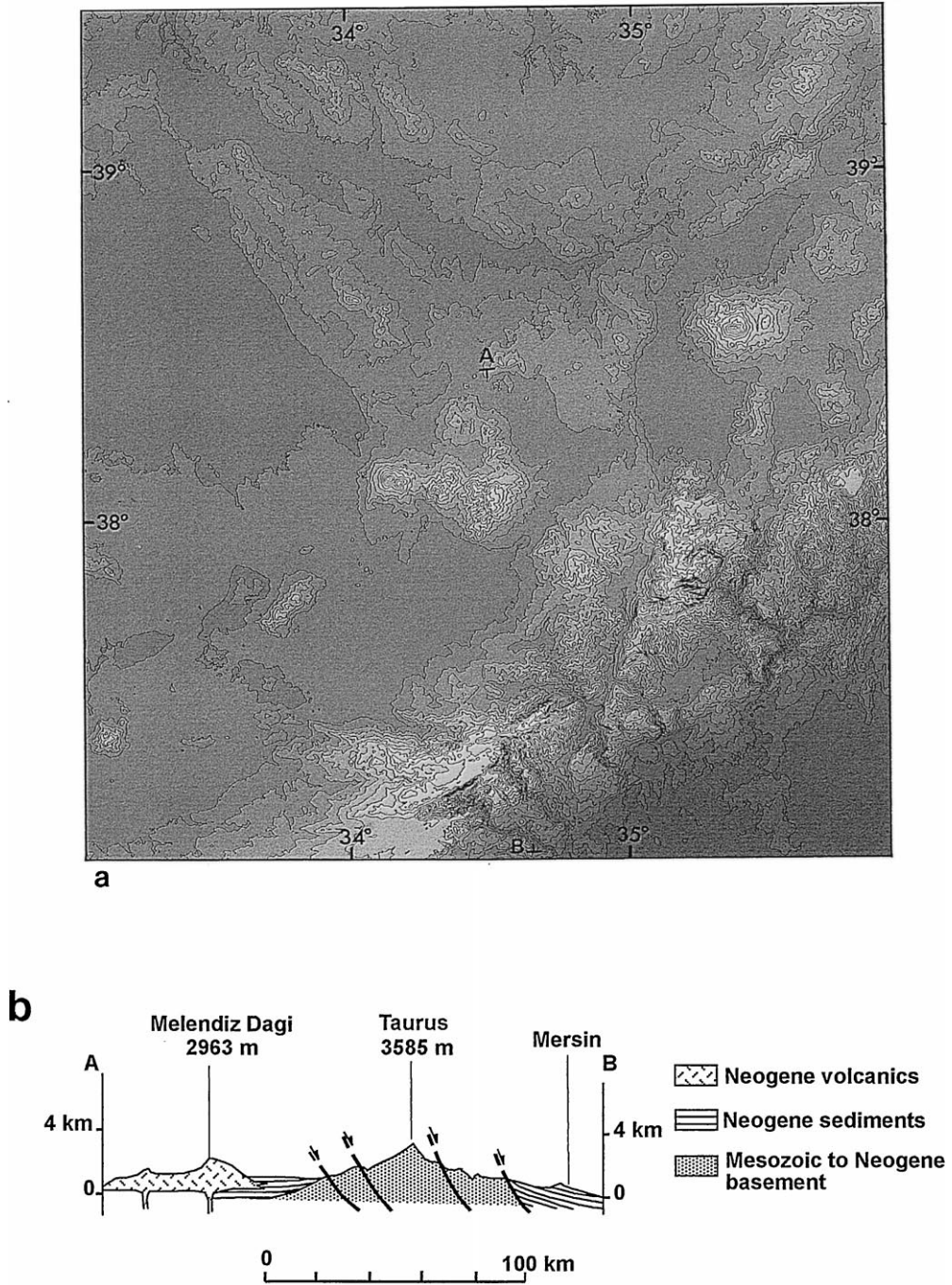


Fig. 12. Relative elevation map of the studied area from DEM. (a) The higher altitudes (clear tones) are in the Central Taurus range, except for the largest volcanoes. (b) Topographic cross-section showing N-dipping tilted blocks and normal faults.

m-deep structure, the Cilicia basin, located between the Adana basin and Cyprus (Evans et al., 1978). Basin formation is related with either a transtensive (Evans et al., 1978) or a transpressive tectonic regime (Jackson and McKenzie, 1984). We interpret the Central Taurus range, where only extension has occurred in the late Neogene, as the uplifted shoulder of the Adana–Cilicia basin, related to thermal effects of lithospheric thinning.

In Central Anatolia, west of the Eceemis fault zone, we have identified no recent compressive structures. We have observed only extension, forming blocks which are moving westward or southwestward relatively to the eastern region (Fig. 9). NW-striking major faults are extensional oblique-slip structures with a dextral throw component. Influence of the Aegean extension (Sengör et al., 1985) can be regarded as the major cause for deformation in the studied area, rather than compression inducing lateral extrusion (McKenzie, 1972; Sengör, 1979).

The Eceemis fault zone, active and subjected to left-lateral strike-slip movements, can be regarded as a transfer fault zone in the extensional pattern of Central Anatolia, separating two regions which major normal faults have different orientations. Movements are almost parallel to the Eceemis fault zone as well along the NE-striking as along the NNE-striking segments. The Sultan Saz releasing bend basin was formed where the fault zone turns from a NE-strike to NNE-strike.

Movements trend west in the Tuz Gölü area (sites 1, 3, 4, 5, 15, 16 and 17, Fig. 9). This can be interpreted to result from the influence of the Aegean back-arc opening. However, in the south (sites 2, 19, 20, 12, 24, 23, 11, 13 and 14, Fig. 9) they turn southwestward and southward. This change may be related to the influence of the Adana–Cilicia basin opening, in the frame of N–S-directed extension affecting the area north of Cyprus. This change in movement orientation is also consistent with the Tuz Gölü fault trace turning southward to the ESE.

Given the relatively small size (50 km) of the region where the change in movement orientation occurs, displacements are likely related more to crustal than to lithospheric deformation. This idea is consistent with the Tuz Gölü basin having no topographic thermal shoulders, despite thick Neogene infill. Thinning associated with the Tuz Gölü basin

consequently seems to concern only the crust, not the whole lithosphere. In addition, we have suggested that the Tuz Gölü fault zone is a detachment which have migrated southwestward from the Gumuskent–Derinkuyu fault line, successively to F2 and F1 faults, and finally to the active Tuz Gölü fault. The arched curved shape in plan view of the faults bordering tilted blocks east of the Tuz Gölü basin, suggests they are listric (spoon faults) and connect in depth with horizontal detachments (Lister et al., 1991). The Tuz Gölü main fault dips gently (65°), implying that connection with detachments is not very deep, i.e., in the crust. This conclusion is important because it implies that deformation in the Central Anatolia plateau is not of lithospheric scale but rather that of crustal blocks moving above sub-horizontal detachment surfaces located in the (lower?) crust, possibly related with the active back-arc Aegean extension in the west.

6. Conclusions

The Central Taurus was affected in the late Neogene by uplifting which we relate to its location on the northern shoulder of the north Cyprus Adana–Cilicia lithospheric scale extensional basins. All our observations concur to show that during the late Miocene to present daytime (the time interval of the volcanic activity accounted for in this paper), extension has dominated throughout the Central Anatolian region. No Neogene compressive structures have been observed whereas extensional Neogene fractures are obvious. The tectonic transport direction is regionally westward, but in the southern sector it changes to SW and S. Part of Central Anatolia seems to be under the influence of the Aegean extension, inducing W-directed movements, but extension north of Cyprus interferes and deviates displacements southwards.

The major result of our study is that regional volcanism in Central Anatolia is associated with extension, not compression. At local scale, volcanic vents can be rooted on tension fractures, forming linear clusters and volcanic ridges, or on tail-crack and horsetail structures, including the volcanoes and the caldera complexes of Cappadocia. Oblique-slip movements along extensional faults may influence emplacement of central volcanoes in releasing bends.

The common characteristics of these structures is to open at local scale and give way to the magma.

McKenzie (1972) first defined Anatolia as an undeformed lithospheric block, laterally extruded. Important deformation and volcanism in the Central Anatolian region are consistent with relative movements using mainly horizontal detachment in the (lower?) crust. The clues for this are: (1) lack of lithospheric thermal uplift of the shoulders of the Tuz Gölü basin; (2) migration with time of the detachment faults east of the basin; (3) change in direction of block movements at regional scale; and (4) exclusive use of local scale brittle crustal structures such as tension fractures and tail-cracks used by magma to reach the surface. The only lithospheric scale feature found in the area is related to thermal uplift of the Central Taurus due to upper mantle thinning and subsequent asthenospheric intrusion, forming the northern shoulder of the north Cyprus Adana–Cilicia lithospheric basin.

Acknowledgements

This work has been funded by both the French CNRS (project PICS) and the Turkish TUBITAK (project YBAG-0078/DPT), with support from the French Embassy in Ankara and the Ministère des Affaires Étrangères in Paris. ERS-1 radar data have been provided by the ESA (project AO.F7) and processing expenses partly supported by the CNES. We are indebted to G. Camus and H. Philip for extensive and helpful reviews of this paper.

References

- Angelier, J., Mechler, P., 1977. Sur une méthode graphique de recherche des contraintes principales également utilisable en tectonique et en séismologie: la méthode des dièdres droits. *Bull. Soc. Géol. Fr.* 19, 1309–1318, (sér. 7).
- Arikan, Y., 1975. The geology and petroleum prospects of the Tuz Gölü Basin. *Maden Tetkik Arama Enst. Miner. Res. Explor. Inst. Turk. Bull. (Foreign Ed)*, Ankara, Vol. 85, 17–37.
- Aydar, E., 1992. Etude volcano-structurale et magmatologique du strato-volcan Hasan Dagi (Anatolie Centrale—Turquie). Thèse, Univ. Clermont-Ferrand II, 213 pp.
- Aydar, E., Gündogdu, M.N., Bayhan, H., Gourgaud, A., 1993. Kapadokya bölgesinin Kuvaterner yasli volkanizmasının volkanik-yapısal ve petrolojik incelenmesi. *Doga Türk Yerbilimleri Dergisi* 3, 25–42.
- Bellier, O., Sebrier, M., 1994. Relationship between tectonics and volcanism along the great Sumatran fault zone deduced by SPOT image analysis. *Tectonophysics* 233, 215–231.
- Biju-Duval, B.J., Dercourt J., Le Pichon, X., 1977. From the Tethys Ocean to the Mediterranean seas: a plate tectonic model of the evolution of western Alpine System. In: Biju-Duval, B., Montadert, L. (Eds.), *Structural History of the Mediterranean Basins*. Ed. Technip, Paris, pp. 143–164.
- Borgia, A., Ferrari, L., Pasquarè, G., 1994. Rifting and spreading of the Cappadocia volcanic plateau, Turkey (abstract). *Int. Volcanol. Congress, IAVCEL*, Ankara.
- Brousse, R., Lefèvre, C., 1990. *Le volcanisme en France*. Masson Publ., Paris, 262 pp.
- Chorowicz, J., Sorlien, C., 1992. Oblique extensional tectonics in the Malawi Rift. *Geol. Soc. Am. Bull.* 104, 1015–1023.
- Chorowicz, J., Luxey, P., Lyberis, N., Carvalho, J., Parrot, J.-F., Yürür, T., Gündogdu, N., 1994a. The Maras Triple Junction (Southern Turkey) based on digital Elevation Model and satellite imagery interpretation. *J. Geophys. Res.* 99 (B10), 20225–20242.
- Chorowicz, J., Collet, B., Bonavia, F., Korme, T., 1994b. Northwest to north-northwest extension direction in the Ethiopian Rift deduced from the orientation of structures and fault-slip analysis. *Geol. Soc. Am. Bull.* 105, 1560–1570.
- Chorowicz, J., Luxey, P., Yürür, T., Rudant, J.-P., Gündogdu, N., Lyberis, N., 1995a. Slip motion estimation along the Ovacik fault near Ercinzan (Turkey) using ERS1 radar image. *Rem. Sens. Environ.* 52, 66–70.
- Chorowicz, J., Koffi, B., Chalah, C., Chotin, P., Collet, B., Poli, J.-T., Rudant, J.-P., Sykioti, O., Vargas, G., 1995b. Possibilités et limites de l'interprétation géologique des images (SAR) ERS-1. *Bull. Soc. Fr. Photogrammétrie et Télédétection* 138 (2), 82–95.
- Chorowicz, J., Bardintzeff, J.M., Rasamimanana, G., Chotin, P., Thouin, C., Rudant, J.P., 1997. An approach using SAR ERS images to relate extension fractures to volcanic vents: examples from Iceland and Madagascar. *Tectonophysics* 271, 263–283.
- Chotin, P., Giret, A., Rampnoux, J.P., Sumarso, S., 1980. L'île de Java, un enregistreur des mouvements tectoniques à l'aplomb d'une zone de subduction. *C.R. Soc. Géol. France* 5, 175–177.
- Dengo, G., Bohnenberger, O., Bonis, S., 1970. Tectonics and volcanism along the Pacific marginal zone of Central America. *Geol. Rundsch.* 59 (3), 1215–1232.
- Deruelle, B., N'ni, J., Kambou, R., 1987. Mount Cameroon: an active volcano of the Cameroon line. *J. Afr. Earth Sci.* 6 (2), 197–214.
- Dewey, J.F., Pitman, W.C. III, Ryan, W.B.F., Bonnin, J., 1973. Plate tectonics and the evolution of the Alpine System. *Geol. Soc. Am. Bull.* 84, 137–3180.
- Dewey, J.F., Hempton, M.R., Kidd, W.S.F., Saroglu, F., Sengör, A.M.C., 1986. Shortening of continental lithosphere; the neotectonics of eastern Anatolia, a young collision zone. In: Coward, M.P., Ries, A.C. (Eds.), *Collision Tectonics*. Imp. Coll. Dep. Geol., London, United Kingdom, *Geol. Soc. Spec. Publ.*, Vol. 19, pp. 3–36.
- Evans, G., Morgan, P., Evans, W.E., Evans, T.R., Woodside,

- J.M., 1978. Faulting and halokinetics in the northeastern Mediterranean between Cyprus and Turkey. *Geology* 6, 392–396.
- Francis, P., 1993. *Volcanoes, A Planetary Perspective*. Oxford Univ. Press, 443 pp.
- Froger, J.-L., Lénat, J.-F., Chorowicz, J., Le Penneç, J.-L., Bourdier, J.-L., Köse, O., Zimitoglu, O., Gündoğdu, N.M., Gourgaud, A., 1998. Hidden calderas evidenced by multisource geophysical data; example of Cappadocian calderas, Central Anatolia. *J. Volcanol. Geotherm. Res.* 85.
- Görür, N., Oktay, F.Y., Seymen, I., Sengör, A.M.C., 1984. Paleotectonic evolution of the Tuz Gölü basin complex, Central Turkey: sedimentary record of a Neo-Tethyan closure. *Geol. Soc. London Spec. Publ.* 17, 467–482.
- Gudmundsson, A., 1995. Infrastructure and mechanics of volcanic systems in Iceland. *J. Volcanol. Geotherm. Res.* 64, 1–22.
- Hamilton, W.H., 1979. Tectonics in the Indonesian region. *U.S. Geol. Prof. Pap.* 1078, 345.
- Innocenti, F., Mazzuoli, R., Pasquarè, G., Radicati-di-Brozo, F., Villari, L., 1975. The Neogene calc-alkaline volcanism of central Anatolia: geochronological data on Kayseri–Nigde area. *Geol. Mag.* 112, 349–360.
- Innocenti, F., Manetti, P., Mazzuoli, R., Pasquarè, G., Villari, L., 1982. Anatolia and North-Western Iran. In: Thorpe, R.S. (Ed.), *Andesites: Orogenic Andesites and Related Rocks*. The Open Univ., Dept. Earth Sci., Milton Keynes, UK, pp. 327–349.
- Jackson, J.A., McKenzie, D.P., 1984. Active tectonics of the Alpine–Himalayan belt between western Turkey and Pakistan. *Roy. Astron. Soc. Geophys. J.* 77, 185–264.
- Joffe, S., Garfunkel, Z., 1987. Plate kinematics of the Circum Red Sea, a reevaluation. *Tectonophysics* 141, 5–22.
- Karig, D.E., Kozlu, H., 1990. Late Palaeogene–Neogene evolution of the triple junction region near Maras, south-central Turkey. *J. Geol. Soc. London* 147, 1023–1034.
- Kelling, G., Gökçen, S.L., Floyd, P.A., Gökçen, N., 1987. Neogene tectonics and plate convergence in the eastern Mediterranean: new data from southern Turkey. *Geology* 15, 425–429.
- Koyaguchi, T., Takada, A., 1994. An experimental study on the formation of composite intrusions from zoned magma chambers. *J. Volcanol. Geotherm. Res.* 59, 261–267.
- Le Penneç, J.-L., Bourdier, J.-L., Froger, J.-L., Temel, A., Camus, G., Gourgaud, A., 1994. Neogene ignimbrites of the Nevşehir Plateau (Central Turkey): stratigraphy, distribution and source constraints. *J. Volcanol. Geotherm. Res.* 63, 59–87.
- Le Pichon, X., Angelier, J., 1979. The Hellenic arc and trench system: a key to the neotectonic evolution of the Eastern Mediterranean area. *Tectonophysics* 60, 1–42.
- Le Pichon, X., Gaulier, J.M., 1988. The rotation of Arabia and the Levant fault system. *Tectonophysics* 153, 271–294.
- Lister, G., Etheridge, M., Symonds, P., 1991. Detachment models for the formation of passive continental margins. *Tectonics* 10, 1038–1064.
- Livermore, R.A., Smith, R.G., 1984. Relative motions of Africa and Europe in vicinity of Turkey. In *Geology of the Taurus Belt*. In: Tekeli, O., Gönçüoğlu, M.C. (Eds.), *Proceedings of an International Symposium on the Geology of the Taurus Belt*. Maden Tetkik ve Arama, Ankara, pp. 1–10.
- Lyberis N., 1985. Tectonic evolution of the North Aegean trough. In: Dixon, J.E., Robertson, A.H.F. (Eds.), *The Geological Evolution of the Eastern Mediterranean*. *Geol. Soc. Lond. Spec. Publ.*, Vol. 17, pp. 709–725.
- Macdonald, G.A., 1972. *Volcanoes*. Prentice-Hall, Englewood Cliffs, NJ, 510 pp.
- Mann, P., Schubert, C., Burke, K., 1990. Review of Caribbean neotectonics. In: Dengo, G., Case, J.E. (Eds.), *The Caribbean Region*. Boulder, Colorado, Geological Survey of America, The Geology of North America, v.H.
- McKenzie, D., 1972. Active tectonics of the Mediterranean region. *Geophys. J. R. Astron. Soc.* 30 (2), 109–185.
- Maden Tetkik ve Arama Enstitüsü (MTA), 1989. Geological map 1/100,000 scale, Aksaray Sheet H 17 and Explanatory Note. *Ins. Min. Res. Explor.*, 14 pp.
- Nakamura, K., 1977. Volcanoes as possible indicators of tectonic stress orientation—principle and proposal. *J. Volcanol. Geotherm. Res.* 2, 1–16.
- Nordlie, B.E., 1973. Morphology and structure of the Western Galapagos volcanoes and a model for their origin. *Geol. Soc. Am. Bull.* 84, 2931–2956.
- N’ni, J., Bonin, B., Brousse, R., 1986. Migration de l’activité magmatique de la ligne du Cameroun: réactivation de segments de failles anciennes du socle panafricain. *C. R. Acad. Sci. Paris* 302 (II), 453–456.
- Ophim, J.A., Gudmundsson, A., 1989. Formation and geometry of fractures, and related volcanism of the Krafla fissure swarm, Northeast Iceland. *Geol. Soc. Am. Bull.* 101, 1608–1622.
- Özgül, N., 1976. Torosların bazı temel jeolojik özellikleri. *Türkiye Jeol. Kur. Bul.* 19, 65–78.
- Pasquarè, G., Ferrari, L., 1993. Rifting and spreading of Cappadocian volcanic plateau, Turkey. *American Geophysical Union Fall Meeting, San Francisco*, V22F-10.
- Pasquarè, G., Poli, S., Vezzoli, L., Zanchi, A., 1988. Continental arc volcanism and tectonic setting in Central Anatolia, Turkey. *Tectonophysics* 146, 217–230.
- Pearce, J.A., Bender, J.F., De Long, S.E., Kidd, W.S.F., Low, P.J., Güner, Y., Saroğlu, F., Yılmaz, Y., Moorbath, S., Mitchell, J.G., 1990. Genesis of collision volcanism in Eastern Anatolia, Turkey. In: Le Fort, P., Pearce, J.A., Pecher, A. (Eds.), *Collision Magmatism*. *J. Volcanol. Geotherm. Res.*, 44 (1–2), 189–229.
- Scott, B., 1981. The Eurasian–Arabian and African continental margin from Iran to Greece. *J. Geol. Soc. London* 136, 269–282.
- Sengör, A.M.C., 1979. The North Anatolian transform fault: its age, offset and tectonic significance. *J. Geol. Soc. Am.* 136, 269–282.
- Sengör, A.M.C., Kidd, W.S.F., 1979. Post-collisional tectonics of the Turkish–Iranian plateau and a comparison with Tibet. *Tectonophysics* 55, 361–376.
- Sengör, A.M.C., Yılmaz, Y., 1981. Tethyan evolution of Turkey; a plate tectonic approach. *Tectonophysics* 75, 181–241.
- Sengör, A.M.C., Görür, N., Saroğlu, F., 1985. Strike-slip faulting

- and related basin formation in zones of tectonic escape: Turkey as a case study. In: Biddle, K.T., Christie-Blick, N. (Eds.), *Strike-Slip Deformation, Basin Formation and Sedimentation*. Soc. Econ. Palaeontol. Mineral. Spec. Publ., 37, 227–264.
- Smith, M., Dunkley, P.N., Deino, A., Williams, L.A.J., McCall, G.J.H., 1995. Geochronology, stratigraphy and structural evolution of Silali volcano, Gregory rift, Kenya. *J. Geol. Soc. London* 152, 297–310.
- Stoiber, R.E., Carr, M.J., 1973. Quaternary volcanic and tectonic segmentation of Central America. *Bull. Volcanol.* 37, 304–325.
- Takada, A., 1994. Development of a subvolcanic structure by the interaction of liquid-filled cracks. *J. Volcanol. Geotherm. Res.* 62, 207–224.
- Temel, A., 1992. Kapadokya eksplosif volkanizmasının petrolojik ve jeokimyasal özellikleri. Doktorat Tezi, Hacettepe Üniversitesi, Fen Bil. Enst., 208 pp.
- Toprak, V., Göncüoğlu, M.C., 1993. Tectonic control on the development of the Neogene–Quaternary Central Anatolian volcanic province, Turkey. *Geol. J.* 28, 357–369.
- Yazgan, E., Chessex, R., 1991. The Malatya Geotraverse and its bearing on tectonics of Eastern Taurus Belt. *Turkey Assoc. Petrol. Geol. Bull.* 3, 1–42.
- Yetis, C., 1984. New observations on the age of the Eceemis Fault. In: Tekeli, O., Göncüoğlu, M.C. (Eds.), *Geology of the Taurus Belt*. Ankara, Turkey, pp. 159–164.
- Yılmaz, Y., 1990. Comparison of young volcanic associations of western and eastern Anatolia formed under a compressional regime: a review. *J. Volcanol. Geotherm. Res.* 44, 69–87.
- Yılmaz, Y., 1993. New evidence and model of the evolution of the southeast Anatolian orogen. *Geol. Soc. Am. Bull.* 105, 252–271.